Chromatic dispersion, nonlinear parameter and modulation formats monitoring based on Godard's error for coherent optical transmission systems

Lin Jiang, Lianshan Yan, Anlin Yi, Yan Pan, Ming Hao, Wei Pan, Bin Luo, Yves Jaouën

Chromatic Dispersion, Nonlinear Parameter, and Modulation Format Monitoring Based on Godard's Error for Coherent Optical Transmission Systems

Lin Jiang,[1] **Lianshan Yan**,[1] ***Senior Member, IEEE***, **Anlin Yi**,[1]
Yan Pan,[1] **Ming Hao**,[1] **Wei Pan**,[1] **Bin Luo**,[1] **and Yves Jaouën**[2]

[1]Center for Information Photonics & Communications, School of Information Science and Technology, Southwest Jiaotong University, Chengdu 610031, China
[2]LTCI, Télécom ParisTech, Université Paris Saclay, Paris 75013, France

Abstract: This paper considers Godard's error as signal quality metric to monitor chromatic dispersion (CD), nonlinear parameter, and modulation format in the DSP module of the coherent receivers. We first review a CD monitoring based on Godard's error that can be able to accurately monitor arbitrarily large dispersion values in uncompensated transmission links in combination with frequency domain equalizer, then extend the previous nonlinear parameter monitoring method based on Godard's error by blindly obtaining the optimized value $\gamma\xi p$ to significantly improve the adaptive capability, and present a simple and effective modulation format monitoring based on Godard's error. Meanwhile, the effectiveness has been experimentally verified in 128-Gb/s PDM-QPSK, 192-Gb/s PDM-8QAM, and 256-Gb/s PDM-16QAM systems.

Index Terms: Digital signal processing, optical performance monitoring, nonlinearity compensation, chromatic dispersion estimation, modulation format monitoring, coherent detection.

1. Introduction

With the development of new broad-bandwidth services such as big data, cloud computing, and social networks, scientists and engineers have spent tremendous efforts to improve the system overall capacity and channel spectral efficiency (SE) to meet the demands of the ever-growing data traffic [1]–[3]. Optical transmission schemes combining different techniques, such as polarization division multiplexing (PDM), advanced modulation formats, coherent detection, as well as digital signal processing (DSP), have been considered or deployed for the next generation large capacity optical networks. In principle, enhanced DSP technology can perfectly compensate for almost all linear impairments such as chromatic dispersion (CD) and polarization mode dispersion (PMD). To facilitate DSP based CD compensation in dynamic optical networks and long haul coherent optical communication systems, it is highly desirable to have accurate and fast chromatic dispersion monitoring scheme which can obtain automatically the accumulated dispersion of transmission link without the information of dispersion parameter and fiber length. So far, various effective CD monitoring and mitigation schemes [4]–[9] have been proposed, including channel estimation based on training symbols, and blind estimation. Additionally, nonlinear Kerr effects including self-phase-modulation (SPM), cross-phase-modulation (XPM) and four-wave-mixing (FWM), are considered as major remaining obstacles in optical coherent transmission systems [10]. Various nonlinearity compensation techniques, such as mid-link optical phase conjugation (OPC) [11], phase-conjugated twin waves [12], Volterra series nonlinear equalizer [13], machine learning techniques [14] and digital back-propagation (DBP) [15]–[20], have been presented for reducing or mitigating nonlinear phase distortions. Among them, DBP algorithm is regarded as one of the most intensively discussed techniques, while it needs to know the full knowledge of link parameters for solving an inverse nonlinear Schrödinger equation. However, in most reconfigurable, dynamic and ultra-long haul systems, link parameters that may vary with time could not be obtained accurately. Therefore, to monitor dynamically link parameters would be highly desirable to guarantee the effectiveness of the DBP algorithm. In [21] a semi-blind DBP has been proposed, where this module is fed with information presumably derived from the signal after detection [22]. Such a solution is unpractical because of the significant delay introduced by the FEC. Subsequently, some blind DBP methods based on phase noise variance and Godard's error [22], [23] have also proposed to estimate nonlinear coefficient γ, while these methods can monitor signal quality before detection. Currently, next generation optical networks will need to be flexible and reconfigurable as network traffic becomes more dynamic and heterogeneous. The key element of flexible networks is the variable transponder that allows network operators to dynamically change signal characteristic such as the data rate, and modulation format according to different link conditions and quality of service requirements. Here, various modulation format monitoring techniques [24]–[26] have also been proposed.

In this paper, we present a series of link or channel information (i.e., CD, nonlinear parameter, modulation format) monitoring methods based on Godard's error. No-knowledge of CD, nonlinear parameter and modulation format need to pre-know, but Godard's error only exploits resources already present in received signals. Here, compared with other CD monitoring methods [6], [7], the CD monitoring method based on Godard's error would present low complexity and wide CD estimation range. In addition, our proposed nonlinear parameter monitoring method may significantly improve the adaptive capability and reduce the time complexity compared with the previous methods [22], [23]. Meanwhile, our modulation format monitoring method utilizes a simple and effective way to identify modulation format with low complexity compared with other methods [24]–[26]. The CD, nonlinear parameter and modulation format monitoring have been experimentally verified in PDM-QPSK, PDM-8QAM PDM-16QAM systems, respectively. The results show that the Godard's error can effectively monitor link or channel information.

2. Theory of Proposed Method

The optical signal propagation in fiber can be approximated by the vector nonlinear Schrödinger equation [16]

$$\frac{\partial E}{\partial z} - \frac{j\beta_2}{2}\frac{\partial^2 E}{\partial t^2} + \frac{\alpha}{2}E = j\gamma|E|^2E \tag{1}$$

where E is the signal envelope, β_2 is dispersion parameter, α is attenuation coefficient, and γ is nonlinear coefficient. In the multiple fiber spans transmission link, each inline amplifier can compensate exactly the loss of each fiber span. As described by the nonlinear Schrödinger equation, the linear and nonlinear effect would degrade the transmission performance seriously. In coherent optical system, the received photocurrents are linearly mapped from the optical field, so that both optical amplitude and phase become available to the receiver's digital processors. Therefore, the fiber linear and nonlinear distortions can be compensated using digital signal processing in coherent receiver. Generally, phase multiplication caused by CD effect presents in frequency domain, while nonlinearity effect is a phase multiplication in time domain.

The basic idea of this paper is to consider Godard's error as signal quality metric to monitor chromatic dispersion, nonlinear parameter, and modulation format in the DSP module. According to [5], [34], the Godard's error defined as

$$\varepsilon = \sum_{n=1}^{N} \left(\left| \left| E[m] \right|^2 - R_{1,2} \right| \right), m = 2n - 1, 2n \tag{2}$$

where $2n$–1 and $2n$ are odd and even samples, $R_{1,2} = |E[m]|^4/|E[m]|^2$ are the corresponding odd and even constant power of signal. For CD or nonlinear parameter monitoring, the received signal $E[m]$ needs to compensate a relatively wide range of dispersion values or nonlinear products, and then we can monitor the Godard's error of the signal $E[m]$ and find the minimum error which corresponds the correct estimation result. For modulation format monitoring, we find that different modulation formats present different Godard's error distributions so that we can directly calculate the Godard's error of the signal $E[m]$ to identify modulation formats.

2.1 Chromatic Dispersion Monitoring Based on Godard's Error

Coherent receivers applying digital filters allow CD equalization in the electrical domain, instead of optical domain compensation by using dispersion compensating fiber (DCF) [27] and Bragg gratings [28]. Meanwhile, since the nonlinear tolerance with respect to both SPM and XPM is severely degraded when online dispersion compensation with DCF is employed, the link without DCF would present better performance [29]–[31]. Several digital filters have been applied to compensate CD either using time domain equalizer (TDE) or frequency domain equalizer (FDE) [4], [32]. In the following, CD monitoring and compensation will be demonstrated on FDE, although these operations can as well be applied to TDE. The residual CD of transmission link can be compensated using CMA-based MIMO equalizer. The all-pass transfer function of FDE is defined as

$$H_{CD} = \exp\left(-j\frac{\lambda^2}{2\pi c}\frac{\omega^2}{2}DL\right) \tag{3}$$

where DL is accumulated CD of transmission link which is equal to the product of dispersion parameter D and transmission length L. ω, c and λ are the angular frequency, the speed of light, and the carrier wavelength, respectively. The impulse response of bulk accumulated CD may spread over hundreds of symbols, and then the case would cause serious intersymbol interference. Taking this into account and observing that the equalizer length for CD equalization can easily reach hundreds of samples at high bit rates (especially for transmission without dispersion compensation), we can utilize the overlap-and-save FDE to reduce the equalizer length [33]. In practice transmission systems, accurate CD compensation would be vital to guarantee the effectiveness of whole DSP algorithms, such as polarization division demultiplexing, timing recovery, frequency offset recovery and carrier phase recovery. Therefore, in the long haul optical communication systems, it is highly desirable to have accurate and fast monitoring algorithm to monitor the total dispersion of transmission link.

As depicted in Fig. 1, a CD monitoring scheme based on Godard's error has been presented to monitor the accumulated CD of transmission link. The received digital signal is transformed by a fast Fourier transform (FFT) and multiplied by the inverse of the transfer function H_{CD} in FDE to realize the CD compensation. In order to monitor the CD values, this scheme firstly needs to scan a wide range of accumulated CD values DL (i.e., 0-ps/nm $\sim$ 40000-ps/nm) with a large stepsize δ_{resc}. Subsequently, a coarse estimation value δ_{estc} with relatively large estimation error is obtained. In order to obtain a relatively accurate estimation value, the second iteration is performed with a small stepsize δ_{resf} in a small range of CD values (i.e., from $\delta_{estc} - \delta_{resc}$ to $\delta_{estc} + \delta_{resc}$). Finally, after the CD compensation, we need to calculate the Godard's error and makes a judgment or decision

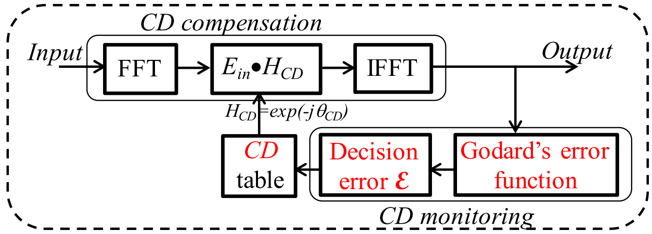

Fig. 1. The principle of the chromatic dispersion monitoring scheme.

whether the Godard's error ε is minimized. Once the minimum error is found, the correct estimation result can be successfully obtained.

2.2 Nonlinear Parameter Monitoring Based on Godard's Error

In recent years, nonlinear effects have been considered as main obstacles in high speed and long haul transmission system. The fiber capacity and transmission distance would be ultimately limited by fiber nonlinear effects. For mitigating or reducing the impact of nonlinear effects, various nonlinear (NL) compensation or mitigation techniques have been mentioned. Among them, DBP algorithm is regarded as one of the most intensively discussed techniques, while it needs to pre-know the full knowledge of link parameters for solving an inverse nonlinear Schrödinger equation. In polarization division multiplexing system, signal propagation in fiber can be simplified by the generalized Manakov equation [16], [17]:

$$\begin{aligned} \frac{\partial E_x}{\partial z} &= -\frac{\alpha}{2}E_x - \frac{i\beta_2}{2}\frac{\partial^2 E_x}{\partial t^2} + \frac{8i\gamma}{9}\left(|E_x|^2 + |E_y|^2\right)E_x \\ \frac{\partial E_y}{\partial z} &= -\frac{\alpha}{2}E_y - \frac{i\beta_2}{2}\frac{\partial^2 E_y}{\partial t^2} + \frac{8i\gamma}{9}\left(|E_y|^2 + |E_x|^2\right)E_y \end{aligned} \tag{4}$$

The Manakov equation can be split into linear and nonlinear parts as follow

$$\frac{\partial E}{\partial z} = \left(\hat{D} + \hat{N}\right)E, \hat{D} = -\frac{i\beta_2}{2}\frac{\partial^2}{\partial t^2}, \hat{N} = \frac{8i\gamma}{9}|E|^2 \tag{5}$$

where $\hat{D}$ and $\hat{N}$ are the dispersion and nonlinear operators. An exact solution of Manakov equation can be approximated by split-step Fourier method (SSFM) which carries out the dispersion operator in two equal parts, before and after the nonlinear operator. Fiber nonlinearity effect can be mitigated or reduced using DBP algorithm which must pre-know or roughly estimate the nonlinear parameter in order to realize precise nonlinear compensation. Nevertheless, due to the difference of material characteristics and manufacturing technology, link information could not be obtained accurately. Therefore, to monitor nonlinear parameter would be highly desirable to guarantee the effectiveness of nonlinear compensation.

A nonlinear parameter monitoring method based on Godard's error has been presented for monitoring the nonlinear parameter as shown in Fig. 2. The digitalized PDM signals (i.e., X and Y) firstly need to carry out the power normalization, and then to recovery the fiber output power p.

$$E_{inx} = X_{nor} \cdot \left|\sqrt{\frac{p}{\text{mean}\left(|X_{nor}|^2\right)}}\right|, E_{iny} = Y_{nor} \cdot \left|\sqrt{\frac{p}{\text{mean}\left(|Y_{nor}|^2\right)}}\right| \tag{6}$$

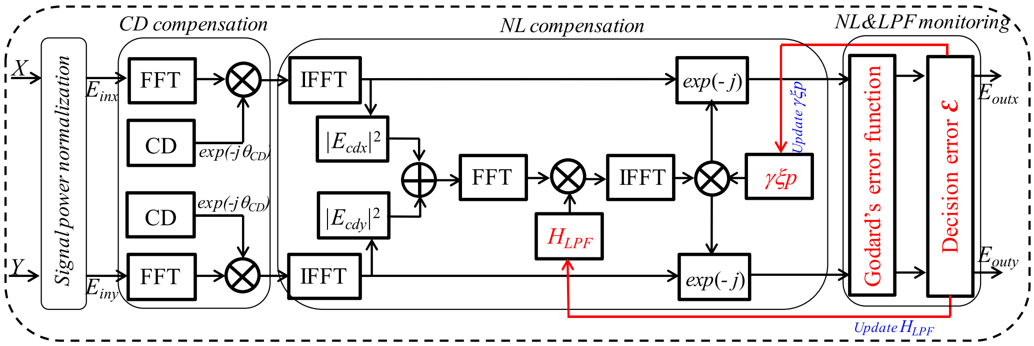

Fig. 2. The principle of the nonlinear parameter and LPF bandwidth monitoring schemes.

where X_{nor}, Y_{nor} are the amplitude normalized signal of X, Y. Next, the digital signals (i.e., E_{inx} and E_{iny}) enter CD compensation module to compensate linear distortions.

$$E_{\text{cdx}} = E_{\text{inx}} \cdot D^{-1} = X_{\text{nor}} \cdot \left| \sqrt{\frac{p}{\text{mean}\left(|X_{\text{nor}}|^2\right)}} \right| \cdot D^{-1}, E_{\text{cdy}} = E_{\text{iny}} \cdot D^{-1} = Y_{\text{nor}} \cdot \left| \sqrt{\frac{p}{\text{mean}\left(|Y_{\text{nor}}|^2\right)}} \right| \cdot D^{-1} \tag{7}$$

where E_{cdx} and E_{cdy} is the signals after CD compensation (D^{-1}). Then, the signals pass though nonlinear compensation module in our previous method [23] which can only estimate nonlinear product $\gamma\xi$ as follow

$$N^{-1} = \exp\left[-j\gamma\xi(P_x + P_y)L_{eff}\right] \tag{8}$$

where γ, ξ, L_{eff} are nonlinear coefficient, compensation factor and the nonlinear effective length of each step, respectively. Here, we aim to improve the adaptive ability of DBP algorithm for achieving multi-parameters estimation. In this paper, the proposed method which is the extended version of previous method can successfully estimate nonlinear operator product $\gamma\xi p$. We can derive from (8) as follows

$$\begin{aligned}\gamma\xi(P_x + P_y) &= \gamma\xi\left[|E_{\text{cdx}}|^2 * \left|\sqrt{\frac{p}{\text{mean}\left(|E_{\text{cdx}}|^2\right)}}\right|^2 + |E_{\text{cdy}}|^2 * \left|\sqrt{\frac{p}{\text{mean}\left(|E_{\text{cdy}}|^2\right)}}\right|^2\right] \\ &= \gamma\xi p\left[\frac{|E_{\text{cdx}}|^2}{\text{mean}\left(|E_{\text{cdx}}|^2\right)} + \frac{|E_{\text{cdy}}|^2}{\text{mean}\left(|E_{\text{cdy}}|^2\right)}\right] = \gamma\xi p\left(|E_X|^2 + |E_y|^2\right)\end{aligned} \tag{9}$$

The proposed nonlinear compensation module can be defined as

$$N^{-1} = \exp\left\{-j\gamma\xi p\left(|E_X|^2 + |E_y|^2\right)L_{eff}\right\} \tag{10}$$

It is worth to note that our proposed method is different from previous method, although they all consider Godard's error as a signal quality metric. The optimum value $\gamma\xi$ of the previous method would change when the receiver end power p fluctuates with the link power fluctuation caused by over- or under-compensation of EDFA. Therefore, if we want to obtain the optimal compensation performance, the optimum nonlinear parameter $\gamma\xi$ needs to be estimated every time. On the contrary, our proposed method use power normalization signals which don't require to receiver end power p before nonlinear compensation in (6). In nonlinear compensation process, we can utilize (10) to directly estimate the optimal nonlinear parameter $\gamma\xi p$. Even if the power p is arbitrarily given, we can also obtain the same, so the optimal nonlinear parameter just needs to estimate only one time.

It is well-known that the nonlinearity of each step is approximated to be lumped at a single point, the phase mismatch effect results in overcompensation of fiber nonlinearity due to high frequency intensity fluctuations. Therefore, a digital LPF, which can limit the bandwidth of the compensating waveform, may be attached in the nonlinear compensator to further improve the compensation performance. Here, the nonlinear compensator is redefined as

$$N^{-1} = \exp\left\{-j\gamma\xi p\left[\mathrm{IFFT}\left[\mathrm{FFT}(|E_x|^2 + |E_y|^2) * H_{\mathrm{LFP}}\right] L_{eff}\right]\right\} \tag{11}$$

The function of LPF can be given by $H_{\mathrm{LFP}} = \exp(-\log_2(f_s/f_c)^2)$, where f_s and f_c are the sample frequency and the filter cutoff frequency, respectively. When the first step is to carry the nonlinear parameter monitoring, the LPF bandwidth needs to set an initial value.

In order to achieve blind monitoring, the nonlinear operator product $f = \gamma\xi p$ is updated according to the steepest descent principle shown as

$$f(i+1) = f(i) + \mu_{\mathrm{adap}}\partial\varepsilon(i) \tag{12}$$

where the adaptive convergence factor μ_{adap} is 0.01. And then, we can monitor the cost function of the Godard's error after the nonlinear compensation. The approach needs to make a judgment or decision whether Godard's error ε is minimized (i.e., $\partial\varepsilon(i) = 0$). The formula $\partial\varepsilon(i)$ is defined as $[\varepsilon(i) - \varepsilon(i-1)]/[f(i) - f(i-1)]$. If it is not minimized, the nonlinearity monitoring approach would continue to update according to (12). If yes, the optimized nonlinear product $\gamma\xi p$ can be obtained. No matter the CD monitoring or the nonlinearity monitoring is carried out before MIMO equalization (polarization division demultiplexing). The monitoring signal would not present modulation format features (i.e., QPSK with one circle and 16QAM with three circles) without polarization division demultiplexing. Therefore, the Godard's error can utilize the constant power instead of the multi-level power to monitor the 16QAM signal. The LPF bandwidth would greatly affect the nonlinear compensation performance. Thus, to adaptively monitor the optimal LPF bandwidth would be necessary highly. As shown in Fig. 2, the nonlinear parameter and LPF bandwidth monitoring methods based on Godard's error has presented. When the nonlinear parameter monitoring process is over, we can obtain the optimized nonlinear product. The subsequent nonlinear compensation can utilize the optimized product to realize the optimal performance. Next, we can begin to monitor the optimal LPF bandwidth. The monitoring approach needs to scan a wide range of bandwidth values. The cost function of the Godard's error after nonlinear compensation would be monitored. When the Godard's error is minimized, the optimal LPF bandwidth would be obtained.

2.3 Modulation Format Monitoring Based on Godard's Error

The constellation diagrams after CMA equalization with different modulation formats (i.e., QPSK, 8QAM, 16QAM) are shown in Fig. 3(a). The CMA equalization aims to compensate almost all linear transmission impairments, and to achieve preliminary demuliplexing which can make the signals more clearly. When we obtain accurate modulation format information, optimal demuliplexing performance can be obtained by using the corresponding MMA algorithm to demultiplex. Here, we calculate the Godard's error of different modulation formats, and then find different Godard's error distributions as shown in Fig. 3(b). We can utilize the unique feature to distinguish modulation formats. The principle of proposed modulation format monitoring scheme is shown in Fig. 3(c).

3. Experimental Results and Discussion

The experimental setup of 128-Gb/s PDM-QPSK, 192-Gb/s PDM-8QAM and 256-Gb/s PDM-16QAM coherent optical transmission systems is shown in Fig. 4. At the transmitter side, a test sequence with a word length of $2^{15}-1$ pseudo-random bit sequence (PRBS) is generated, and needs to map into *m*QAM modulation format with 2 samples per symbol. The up-sampled signals are shaped by using a square root raised cosine (SRRC) with a roll-off factor of 1.0. Next, a pre-distortion operation is utilized to overcome the frequency roll-off of a digital to analog converter (DAC). The light from an external cavity laser (ECL) at ~1550-nm with ~100-kHz linewidth

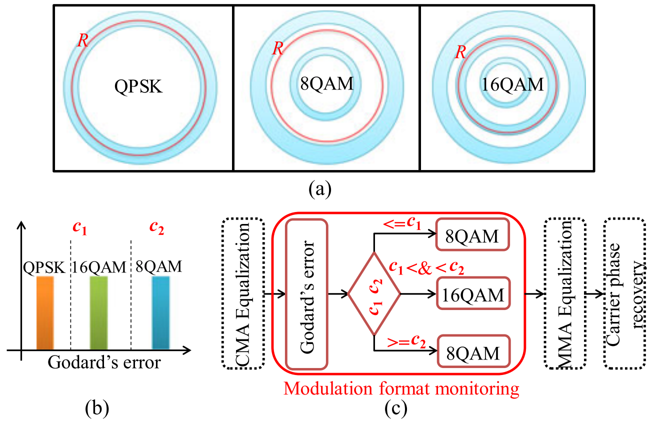

Fig. 3. (a) The constellation of QPSK, 8QAM and 16QAM after CMA demultiplexing with constant power R. (b) The Godard's error distributions of different modulation formats. (c) The principle of modulation format monitoring scheme.

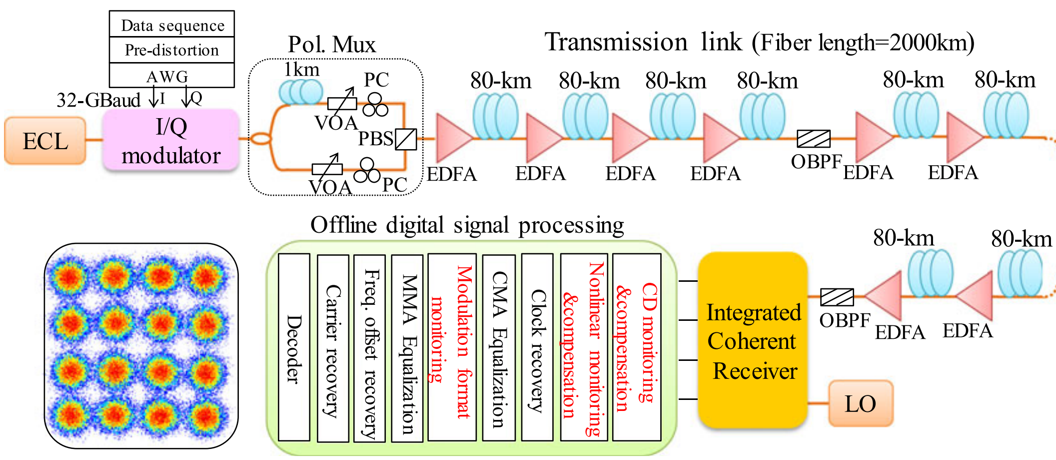

Fig. 4. Experimental setup of the 128-Gb/s PDM-QPSK, 192-Gb/s PDM-8QAM and 256-Gb/s PDM-16QAM systems. ECL: External Cavity Laser; VOA: Variable Optical Attenuator; PBS: Polarization Beam Splitter; PC: Polarization Controller; EDFA: Erbium Doped Fiber Amplifier; LO: Local Oscillator.

is modulated by an IQ modulator which is driven by the DAC operating at 64-GSa/s and 25-GHz analog bandwidth. The modulated signals are polarization multiplexed to generate 128-Gb/s PDM-QPSK,192-Gb/s PDM-8QAM and 256-Gb/s PDM-16QAM employing a interleave scheme that is composed of a coupler, two polarization controllers (PCs), two variable optical attenuators (VOAs), 1-km single mode fiber (SMF), and a polarization beam splitter (PBS) to recombine the signals. The transmission optical link is composed of multi-spans SMF whose dispersion parameter, attenuation, and nonlinear coefficient are D $=$ 16.9-ps/nm/km, $\alpha = 0.2$-dB/km, $\gamma = 1.27$-km$^{-1}\cdot$W^{-1}, respectively. Fiber loss of each span is compensated using an erbium doped fiber amplifier (EDFA) with a noise figure of $\sim$5-dB. An optical band-pass filter (OBPF) in link is used to filter amplified spontaneous emission (ASE) noise. At the coherent intradyne receiver side, the signal and the LO are combined at the 90° polarization-and-phase diversity hybrid, and then photo detected by the balanced photo-detector (BPD). The output electrical signals are sampled at 80-GSamples/s by real-time digital oscilloscope with 33-GHz electrical bandwidth. Finally, the digital signals are processed in the off-line digital signal processing module including CD monitoring and compensation, nonlinearity monitoring and compensation followed by time-domain clock recovery. Then the residual CD and polarization mode dispersion (PMD) can be compensated using a 21-tap T/2 spaced

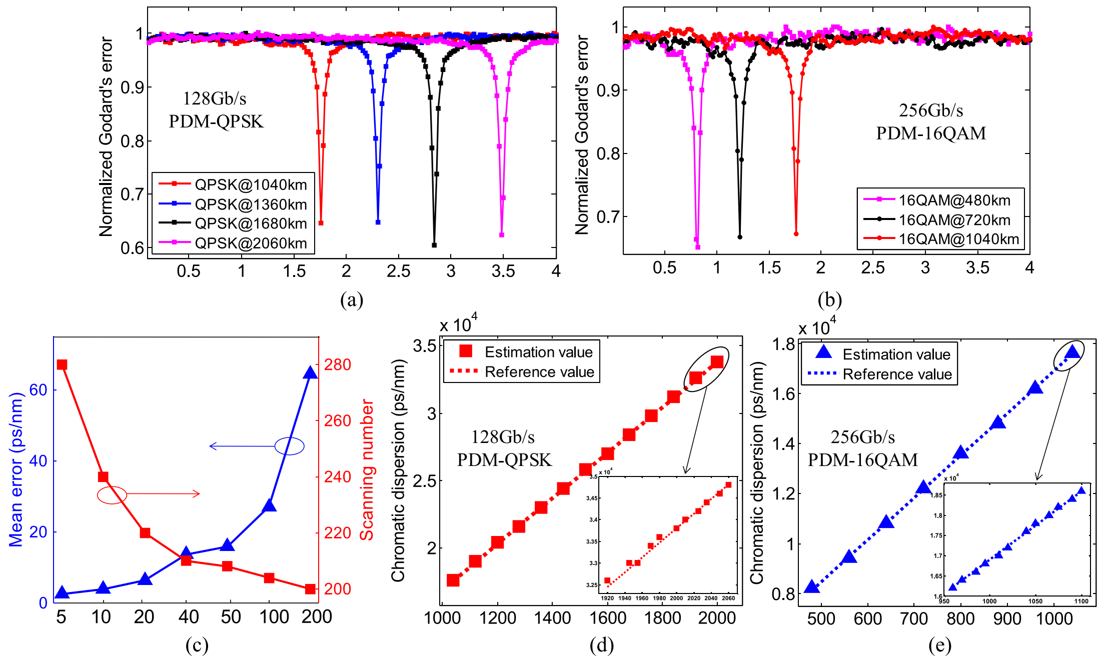

Fig. 5. (a) Normalized Godard's error versus chromatic dispersion for 128-Gb/s PDM-QPSK with 1040-km, 1360-km, 1680-km, 2000-km. (b) Normalized Godard's error versus chromatic dispersion for 256-Gb/s PDM-16QAM with 480-km, 720-km, 1040-km. (c) The mean error of CD monitoring and scanning numbers with different stepsizes. (d) The CD monitoring results of 128-Gb/s PDM-QPSK with a range from 1040-km to 2060-km. (e) The CD monitoring results of 256-Gb/s PDM-16QAM with a range from 480 km to 1040-km.

butterfly equalizer based on constant-modulus algorithm (CMA) equalization. Meanwhile, the digital signals can achieve preliminary demuliplexing. Next, we need to utilize modulation format monitoring module for obtaining accurate modulation format information. Once we know the modulation format, we can choose the corresponding MMA algorithm to demultiplex. The frequency offset and carrier phase recovery modules are utilized to compensate laser frequency shift and phase noise. Finally, the data decision module is applied to evaluate the system performance by counting the bit errors.

To blindly monitor accumulated CD of transmission link, the proposed scheme needs to scan the CD value of the FDE with a wide range (i.e., $0 \sim 40000$-ps/nm). After scanning the CD value, the scheme monitors the cost function of the normalized Godard's error to find the minimum Godard's error as shown in Fig. 5(a) and (b). The minimum Godard's error corresponds to the CD value which can be considered as the accumulated CD value of transmission link. The monitoring CD value can be used to set CD equalizer to compensate the impairments caused by CD. The Godard's error monitoring curves for 128-Gb/s PDM-QPSK and 256-Gb/s PDM- 16QAM are shown in Fig. 5(a) and (b) with different fiber lengths (1040-km, 1360-km, 1680-km, 2060-km), and (480-km, 720-km, 1040-km), respectively. As can be seen, there are different minimum Godard's error values with different fiber lengths. When the fiber length of the link is 1040 km corresponding to chromatic dispersion value $\sim$17576-ps/nm, the QPSK and 16QAM signals can obtain the same CD values. Certainly, the normalized Godard's error of 16QAM would be higher slightly than that of QPSK, since a 16QAM signal has more amplitude levels than a QPSK signal. The mean error of CD monitoring with different stepsizes varying from 5- to 200-ps/nm for 128-Gb/s PDM-QPSK system in the presence of 1040 to 2060-km fiber length are shown in Fig. 5(c). Meanwhile, we also calculate the total scanning number which corresponds to running time of CD monitoring. Here, we just consider the influence of the stepsize δ_{resf} of the second iteration which is related to the CD estimation accuracy so that we assume that the stepsize δ_{resc} of the first iteration is 200-ps/nm.

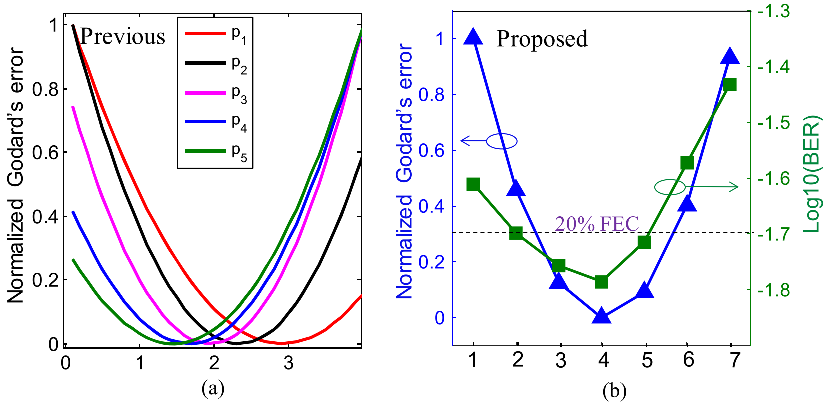

Fig. 6. (a) The normalized Godard's error with different powers based on previous work for PDM-16QAM. (b) The normalized Godard's error and the corresponding BER by using the present method for PDM-16QAM.

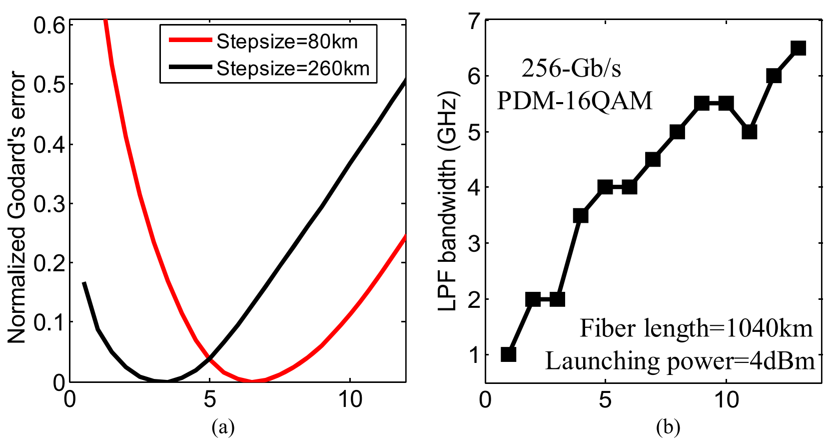

Fig. 7. (a) The normalized Godard's error with the different bandwidths under different nonlinear compensation stepsizes (i.e., 80-km, 260-km). (b) The optimal bandwidth with the different numbers of steps.

The mean error of each stepsize is calculated based on 50 independent experiments. We can see that the mean error increases when the stepsize becomes large, while the scanning number can be reduced significantly. Here, after weighting the scanning number and the stepsize, we choose an optimal stepsize δ_{resf} 40-ps/nm in this paper. As shown in Fig. 5(d) and (f), we monitor the accumulated CD value of different modulation formats with different fiber lengths. As can be seen, the scheme can monitor a wide range of the transmission link (i.e., from 1040-km to 2060-km), also be effective to a small link resolution 10-km (i.e., 2025-km, 2035-km, 2050-km). The estimation value is close to the reference value within a small fluctuation as shown in Fig. 5(d) and (f).

Before nonlinear parameter monitoring, we need to set an initial LPF bandwidth in (11) to compensate nonlinear effect. As shown in Fig. 6(a), the optimal product $\gamma\xi$ of previous method would change when the receiver end power p (p_1, p_2, p_3, p_4, p_5) fluctuates with the link power fluctuation caused by the under- or over-compensation of node amplifier. Therefore, the previous method needs to estimate optimal product $\gamma\xi$ every time for obtaining the optimal compensation performance. In our proposed method, even if the power p presents different values, we can also obtain the same optimal value $\gamma\xi p$, so the optimal nonlinear parameter just needs to estimate only one time as shown in Fig. 6(b). For verifying the accuracy of Godard's error, the corresponding BER

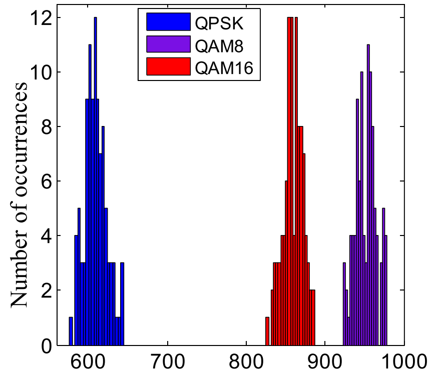

(a)

Modulation format identification			
	QPSK	8QAM	16QAM
QPSK	97.875%	/	2.1250%
8QAM	/	99.778%	0.222%
16QAM	/	1.769%	98.231%

(b)

Fig. 8. (a) The Godard's error distributions of three modulation formats. (b) Dentification accuracies for various modulation formats.

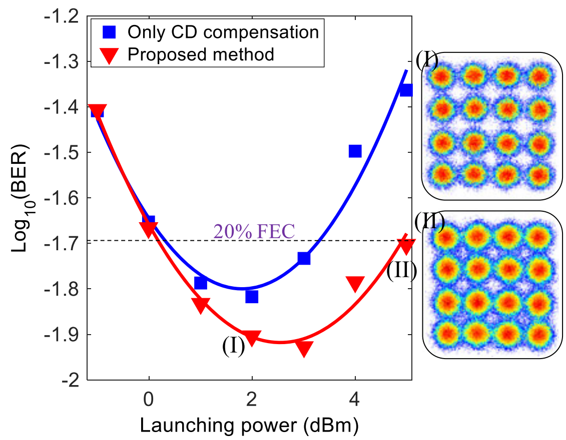

Fig. 9. BER as a function of optical launching power with fiber length 1040-km for 256-Gb/s PDM-16QAM signals.

performance has been calculated as shown in Fig. 6(b). The results show that the monitoring product $\gamma\xi p$ is the same.

When the optimal value $\gamma\xi p$ is obtained, we can further monitor the optimal LPF bandwidth for improving the compensation performance. A wide range of bandwidth values need to be swept, and then the normalized Godard's error would be monitored for finding the minimum Godard's error. Here, different nonlinear compensation stepsizes (i.e., 80-km, 260-km) can obtain different optimal LPF bandwidths for 256-Gb/s PDM-16QAM system as depicted in Fig. 7(a). For instance, when the nonlinear compensation stepsize is 80-km, the optimal LPF bandwidth is ∼6.5-GHz. Therefore, we need to first perform the nonlinear parameter monitoring which would decide the stepsize for obtaining the better compensation performance. And then, the optimal LPF bandwidth can be determined. We then calculate the optimal bandwidths with the different numbers of stepsizes as depicted in Fig. 7(b). The larger nonlinear compensation stepsize are used, the smaller LPF bandwidth is needed for obtaining optimal performance.

As shown in Fig. 8(a), the different modulation formats after CMA equalization show different Godard's error distributions. We can distinguish these modulation formats using unique feature. Here, all modulation formats use 3000 symbols to calculated Godard's error. To verify the reliability of identification performance, the OSNR interval utilizes 0.5-dB, and each OSNR value is implemented with 100 independent implementations. The OSNRs of PDM-QPSK, PDM- 8QAM, PDM-16QAM signals are altered in the ranges of 12 ∼ 17.5-dB, 16.5 ∼ 22.5-dB, 18.5 ∼ 24.5-dB, respectively.

The detailed identification accuracies for various modulation formats using the proposed method as depicted in Fig. 8(b). The accuracies of QPSK, 8QAM and 16QAM are 97.875%, 99.778% and 98.231%, respectively. The modulation format identification based on Godard's error is a simple and effective method.

To further investigate the performance of proposed method, the BER performance of the present method in different launching powers is calculated for 256-Gb/s PDM-16QAM signals with 1040-km fiber length as shown in Fig. 9. The proposed method with optimal CD value, optimal nonlinear parameter, and correct modulation format identification can perform better than only CD compensation. Meanwhile, the corresponding constellations are inserted in Fig. 9.

4. Conclusion

We consider Godard's error as signal quality metric to monitor chromatic dispersion, nonlinear parameter, and modulation format in the DSP module of the coherent receivers. In this paper, we review a chromatic dispersion monitoring based on Godard's error, extend our previous nonlinear parameter monitoring method by adaptively gaining the optimized value $\gamma\xi p$ to significantly improve the adaptive capability, and present a simple and effective modulation format monitoring method. The effectiveness is demonstrated experimentally in PDM-QPSK, PDM- 8QAM, and PDM-16QAM systems. In the future transmission network, it is a very strong desire to blindly monitor link or channel information. Meanwhile, note that we only consider the single channel case with SPM effects. It is desirable to investigate the performance of multi-channel case with SPM, XPM and FWM effects in the near future.

References

[1] P. Winzer, "Beyond 100 G ethernet," *IEEE Commun. Mag.*, vol. 48, no. 7, pp. 26–30, Jul. 2010.

[2] L. Yan, X. Liu, and W. Shieh, "Toward the Shannon limit of spectral efficiency," *IEEE Photon. J.*, vol. 3, no. 2, pp. 325–330, Apr. 2011.

[3] A. D. Ellis, J. Zhao, and D. Cotter, "Approaching the non-linear Shannon limit," *J. Lightw. Technol.*, vol. 28, no. 4, pp. 423–433, Feb. 2010.

[4] R. Soriano, F. N. Hauske, N. Gonzalez, Z. Zhang, Y. Ye, and I. Monroy, "Chromatic dispersion estimation in digital coherent receivers," *J. Lightw. Technol.*, vol. 29, no. 11, pp. 1627–1637, Jun. 2011.

[5] M. Kuschnerov, F. N. Hauske, K. Piyawanno, B. Spinnler, A. Napoli, and B. Lankl, "Adaptive chromatic dispersion equalization for nondispersion managed coherent systems," in *Proc. Opt. Fiber Commun.*, San Diego, CA, USA, 2009, Paper OMT1.

[6] D. Wang, C. Lu, A. P. T. Lau, and S. He, "Adaptive chromatic dispersion compensation coherent communication systems using delay-tap sampling technique," *IEEE Photon. Technol. Lett.*, vol. 23, no. 14, pp. 1016–1018, Jul. 2011.

[7] C. C. Do *et al.*, "Chromatic dispersion estimation in 40 Gb/s coherent polarization-multiplexed sinigle carrier system using complementary Golay sequences," in *Proc. Opt. Fiber Commun.*, Los Angeles, CA, USA, 2012, Paper OW4G.1.

[8] C. Xie, "Chromatic dispersion estimation for single-carrier coherent optical communications," *IEEE Photon. Technol. Lett.*, vol. 25, no. 10, pp. 992–995, May. 2013.

[9] L. Jiang *et al.*, "Fast and adaptive chromatic dispersion compensation scheme for digital coherent systems utilizing two-stage estimation," *Opt. Exp.*, vol. 23, no. 12, pp. 16177–16183, Jun. 2015.

[10] J. C. Cartledge *et al.*, "Signal processing techniques for reducing the impact of fiber nonlinearities on system performance," in *Proc. Opt. Fiber Commun.*, Anaheim, CA, USA, 2016, Paper Th4F.5.

[11] S. Kumar and L. Liu, "Reduction of nonlinear phase noise using optical phase conjugation in quasi-linear optical transmission," *Opt. Exp.*, vol. 15, no. 5, pp. 2166–2177, Mar. 2007.

[12] X. Liu, A. R. Chraplyvy, P. J. Winzer, R. W. Tkach, and S. Chandrasekhar, "Phase-conjugated twin waves for communication beyond the Kerr nonlinearity limit," *Nature Photon.*, vol. 7, no. 7, pp. 560–568, 2013.

[13] F. P. Guiomar and A. N. Pinto, "Simplified Volterra series nonlinear equalizer for polarization-multiplexed coherent optical systems," *J. Lightw. Technol.*, vol. 31, no. 23, pp. 3879–3891, Dec. 2013.

[14] D. Zibar, M. Piels, R. Jones, and C. G. Schäeffer, "Machine learning techniques in optical communication," *J. Lightw. Technol.*, vol. 34, no. 6, pp. 1442–1452, Mar. 2016.

[15] E. Ip and J. M. Kahn, "Compensation of dispersion and nonlinear impairments using digital backpropagation," *J. Lightw. Technol.*, vol. 26, no. 20, pp. 3416–3425, Oct. 2008.

[16] F. Yaman and G. Li, "Nonlinear impairment compensation for polarization-division multiplexed WDM transmission using digital backward propagation," *IEEE Photon. J.*, vol. 2, no. 5, pp. 816–832, Oct. 2010.

[17] D. Rafique, J. Zhao, and A. D. Ellis, "Digital back-propagation for spectrally efficient WDM 112Gbit/s PM m-ary QAM transmission," *Opt. Exp.*, vol. 19, no. 6, pp. 5219–5224, Mar. 2011.

[18] L. B. Du and A. J. Lowery, "Improved single channel back propagation for intra-channel fiber nonlinearity compensation in long-haul optical communication systems," *Opt. Exp.*, vol. 18, no. 16, pp. 17075–17088, Jul. 2010.

[19] L. Jiang *et al.*, "Toward blind nonlinearity estimation in back-propagation algorithm for coherent optical transmission systems," in *Proc. Opt. Fiber Commun.*, Los Angeles, CA, USA, 2017, Paper W1G.3.
[20] A. Amari, O. A. Dobre, R. Venkatesan, O. S. Kumar, P. Ciblat, and Y. Jaouen, "A survey on fiber nonlinearity compensation for 400 Gbps and beyond optical communication systems," *IEEE Commun. Surveys Tuts.*, vol. 19, no. 4, pp. 3097–3113, Oct–Dec. 2017.
[21] T. Tanimura *et al.*, "Semi-blind nonlinear equalization in coherent multi-span transmission system with inhomogeneous span parameters," in *Proc. Opt. Fiber Commun.*, Los Angeles, CA, USA, 2010, Paper OMR.6.
[22] C. Lin *et al.*, "Adaptive digital back-propagation for optical communication systems," in *Proc. Opt. Fiber Commun.*, Los Angeles, CA, USA, 2010, Paper M3C.4.
[23] L. Jiang *et al.*, "Low complexity and adaptive nonlinearity estimation module based on Godard's error," *IEEE Photon. J.*, vol. 8, no. 1, Feb. 2016, Art. no. 7801007.
[24] P. Isautier, J. Pan, R. DeSalvo, and S. Ralph, "Stokes space-based modulation format recognition for autonomous optical receivers," *J. Lightw. Technol.*, vol. 33, no. 24, pp. 5157–5163, 2015.
[25] T. Bo, J. Tang, and C. Chan, "Modulation format recognition for optical signals using connected component analysis," *IEEE Photon. Technol. Lett.*, vol. 29, no. 1, pp. 11–14, Jan. 2017.
[26] R. Boada, R. Borkowski, and I. Monroy, "Clustering algorithms for Stokes space modulation format recognition," *Opt. Exp.*, vol. 23, no. 12, pp. 15521–15531, 2015.
[27] L. Gruner-Nielsen *et al.*, "Dispersion compensating fibers," *J. Lightw. Technol.*, vol. 23, no. 11, pp. 3566–3579, Nov. 2005.
[28] F. Ouellette, J. F. Cliche, and S. Gagnon, "All-fiber devices for chromatic dispersion compensation based on chirped distributed resonant coupling," *J. Lightw. Technol.*, vol. 12, no. 10, pp. 1728–1738, Oct. 1994.
[29] X. Liu, F. Buchali, and R. W. Tkach. "Improving the nonlinear tolerance of polarization-division-multiplexed CO-OFDM in long-haul fiber transmission," *J. Lightw. Technol.*, vol. 27, no. 16, pp. 3632–3640, Aug. 2009.
[30] C. Xie, "Fiber nonlinearities in 16QAM transmission systems," in *Proc. Eur. Conf. Opt. Commun.*, Geneva, Switzerland, 2011, Paper We.7.B.6.
[31] K. Forozesh, S. L. Jansen, S. Randel, I. Morita, and H. Tanaka, "The influence of the dispersion map in coherent optical OFDM transmission systems," in *Proc. Digest IEEE/LEOS Summer Top. Meetings*, 2008, Paper WC2.4.
[32] B. Spinnler, "Equalizer design and complexity for digital coherent receivers," *IEEE J. Quantum Electron.*, vol. 16, no. 5, pp. 1180–1192, Oct. 2010.
[33] R. Kudo, T. Kobayashi, K. Ishihara, Y. Takatori, A. Sano, and Y. Miyamoto, "Coherent optical single carrier transmission using overlap frequency domain equalization for long-haul optical systems," *J. Lightw. Technol.*, vol. 27, no. 16, pp. 3721–3728, Aug. 2009.
[34] D. Godard, "Self-recovery equalization and carrier tracking in two-dimensional data communication systems," *IEEE Trans. Commun.*, vol. 28, no. 11, pp. 1867–1875, Nov. 1980.